UDC: 544.228

COMPARATIVE ANALYSIS OF ELECTROCHROMIC PROPERTIES OF $CuWO_4$•WO_3, Bi_2WO_6•WO_3 AND WO_3 THIN FILMS

V.O. Smilyk, S.S. Fomanyuk*, I.A. Rusetskyi, M.O. Danilov, G.Ya. Kolbasov

V.I. Vernadskii Institute of General and Inorganic Chemistry of the Ukrainian NAS,
Palladina prospect 32–34, Kyiv 03142, Ukraine;
** e–mail: fomanyuk@gmail.com*

Received 31.06.2022
Accepted 03.09.2022

Abstract: *A comparative analysis of electrochromic properties of composites $CuWO_4$•WO_3, Bi_2WO_6•WO_3 and WO_3 films obtained by electrochemical and chemical methods was carried out. The study into the kinetics of light transmission and spectral characteristics of electrochromic coloration revealed some differences in electrochromic processes. It found that in the WO_3, Bi_2WO_6•WO_3, $CuWO_4$•WO_3 series, lithium intercalation in the film is slowed down, which is due to diffusion limitations in the process of coloring of the Bi and Cu oxides. Spectral characteristics of light transmission Bi_2WO_6•WO_3 and $CuWO_4$•WO_3 also differ from WO_3 in that the contribution to light absorption is also made by Bi and Cu oxides, which are partially reduced by lithium in the process of their coloring. It is shown that the metal tungstates can be effective electrochromic materials with an additional absorption band in the visible region.*
Keywords: *electrochromism, metal tungstates, electrochromic composites*.
DOI: 10.32737/2221-8688-2022-3-289-296

Introduction

There is not enough published studies about electrochromic properties of metal tungstates what delays their use in real devices as smart windows, multicolor bistable displays, solar heat regulation, optical telecommunications and applications in aerospace and military camouflage [1-5]. In this article, thin films of $CuWO_4$•WO_3 and Bi_2WO_6•WO_3 were selected as objects of research into the electrochromic properties of metal tungstates. The tungstates of these metals can have similar spectral characteristics of electrochromic coloration to tungsten oxide with some differences typical for these materials. For the synthesis of films, preference was given to electrodeposition methods with interference control of film thickness. According to the literature analysis, the method of electrochemical deposition provides films with a high degree of hydration [6, 7] and allows controlling the thickness [8] and surface morphology [9] of films, while the choice of the optimal thickness in the range of 150 - 200 nm [10, 11] allows, in turn, expecting the most optimal parameters of electrochromic efficiency and coloration rate.

Experimental part

$CuWO_4$•WO_3 films were obtained in two stages by Cu_2O electrochemical deposition at the cathode current 1 mA/cm^2 from solution of the composition ($CuSO_4$- 0.05 mol/l, citric acid and 2 mol/l KOH, pH = 10) and followed by anodized Cu_2O in a solution of 1 mol/l K_2WO_4 at a voltage of 3.5 V for 0.5 hours. The peroxide electrolyte Na_2WO_4 -0.1 mol/l, H_2O_2 - 0.2 mol/l and H_2SO_4 (pH = 1.1) was used to obtain WO_3 film. The deposition was carried out in the galvanostatic mode with a cathodic current of 1.5 mA/cm^2. Bismuth tungstate was taken off by electrochemical precipitation from an electrolyte containing Bi_2O_3= 45 g/l,

Na_2WO_4 = 100 g/l, 35% H_2O_2 - 50 ml/l, adjusted to pH = 1 with nitric acid (55 ml) at a cathodic current of 1 mA/cm^2. Bismuth tungstate was also obtained by ion layering using solutions of Bi_2O_3 = 45 g/l, pH = 1 (nitric acid 55 ml) and Na_2WO_4 = 100 g/l. All used chemical reagents were analytical grade purchased from Sigma-Aldrich. The XRD study of films was performed using a DRON 4 diffractometer. The optical properties of the films were studied using a Perkin Elmer UV – Vis Lambda 35 spectrophotometer.

The electrochemical measurements of deposited films were performed using PGSTAT Elins P-8S Potentiostat. Platinum was used as a counter electrode and SnO_2 / glass substrate as working electrode. The EC study was carried out in 1 M $LiClO_4$ in propylene carbonate solutions. The change in the light transmittance (electrochromic color) of the films was measured using a universal setup based on a single-beam diffraction spectrophotometer of the C-302 type, which provided measurements in the wavelength range λ from 300 to 1300 nm. The monochromator was controlled using a complex based on a personal computer. The galvanostatic current change was provided with the help of the G6-26 signal generator, which supplies a current control pulse to the potentiostat and electrochromic cell. At the same time, the dynamics of changes in the intensity of the transmitted light through the film were recorded.

Results and discussion

The mechanism of electrochemical formation of Bi_2WO_6 films is similar to the processes of formation of WO_3 as a result of electroreduction of peroxide-complex compounds based on tungstate ions. The interaction of Na_2WO4 and H_2O_2 forms a peroxotungstate complex $[(O_2)_2(O)W–O–W(O)(O_2)_2]^{2-}$ [12]. The work [13] shows that the process of electrodeposition of WO_3 from acidic solutions containing this complex is carried out in two stages: 1 – electrochemical breaking of the O-O bond in the molecule of the peroxotungstate complex and 2 – the chemical stage of polymerization to tungstic acid that forms tungstate ions ($H_2WO_4=WO_4^{2-}+2H^+$) and is present in the near-cathode space. If ions (Bi^{3+}) are added to the deposition solution, along with the formation of H_2WO_4 the Bi_2WO_6 will also be co-precipitated. Studies of the structure of the obtained films proved this assumption. From the interpretation of X-rays, fig. 1, it is established that along with Bi_2WO_6, hydrated phases of WO_3 are also observed. Fig. 1 presents the results of X-ray phase analysis of bismuth tungstate obtained by ion layering (a) and electrochemical method (b). X-ray diffraction analysis established that the composition of the materials is mixed and includes, in addition to bismuth orthorhombic tungstate, tungsten trioxide with a hexagonal structure. The comparison of X-ray phase analysis for chemically and electrochemically obtained Bi_2WO_6 showed that the films obtained by electrochemical deposition have an amorphous structure, with interspersed crystallites of orthorhombic Bi_2WO_6 and hexagonal WO_3 (Fig. 1 (b)) [14, 15], while the films obtained by ion layering have a polycrystalline structure with broadened peaks (Fig. 1 (a), which indicates the fine-grained nature of the obtained crystallites. This is explained as being due to the fact that during ion layering, crystal points are created for further crystal growth, and during electrochemical deposition, a process similar to polymerization takes place following which an amorphous mixture of mixed phase composition Bi_2WO_6•WO_3 is formed. To obtain thin $CuWO_4$•WO_3 films with optimal electrochromic parameters [10, 11], voltammetric studies of Cu_2O electrodeposition as a precursor for the formation of $CuWO_4$•WO_3 were performed. The choice of Cu_2O current electrodeposition is based on voltammetric studies. Fig. 2 shows voltammetry of the Cu_2O precipitation process from citrate solution based on $CuSO_4$ and alkali. From the analysis of the curve of Fig. 2 it was found that within the potentials of the reduction wave from Cu^{2+} to Cu^+ [16] the current is 1 mA/cm^2. As a result, Cu_2O films are formed.

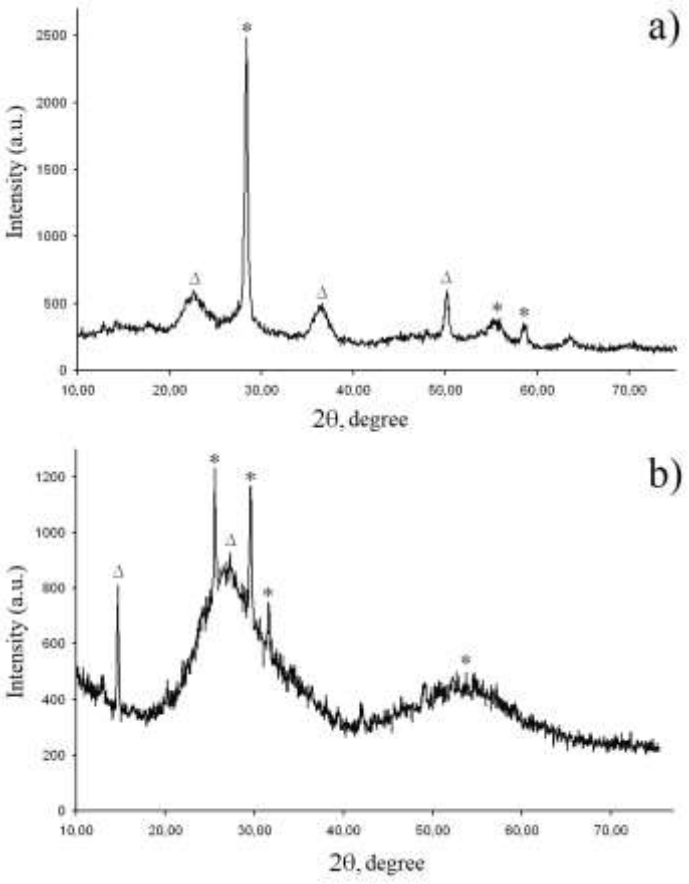

Fig.1. a - XRD pattern of chemically obtained bismuth tungstate, where *– orthorhombic Bi_2WO_6, Δ – hexagonal WO_3; b - X-ray phase analysis of electrochemically obtained bismuth tungstate.

The resulting Cu_2O films were anodized in 1 mol / l K_2WO_4 solution at 3.5 V for 30 min. The anodization resulted in the dissolution of Cu_2O and the formation of $CuWO_4$ sediment. The process of anodizing Cu_2O can be described by reactions [17] as follows:

$$Cu_2O + H_2O = 2Cu^{2+} + 2OH^- + 2e^- \quad (1)$$

$$WO_4^{2-} + Cu^{2+} = CuWO_4 \quad (2)$$

Upon completion of these reactions, thin films of $CuWO_4$ copper tungstate with WO_3 impurities were obtained. In parallel with the $CuWO_4$ formation there is the reaction of water decomposition at the anode with the release of oxygen and H^+ protons that interact with WO_4^{2-} to form hydrated forms of WO_3:

$$2H_2O = 4H^+ + O_2 + 4e^- \quad (3)$$

$$WO_4^{2-} + 2H^+ = WO_3 \cdot H_2O \quad (4)$$

X-ray phase analysis $CuWO_4$•WO_3 on the Fig. 3 showed the presence of monoclinic structure $CuWO_4 \cdot 2H_2O$ (standard card (PDF 33-0503)) [18,19] and undeciphered tungstate structure, possibly, phase $CuWO_4$ (standard card (JCPDS No 88-0269)) [20] with impurities of hydrated forms WO_3 monoclinic WO_3•$2H_2O$ (JCPDS Card No.18-1420) [21], orthorhombic WO_3•$0.33H_2O$ (JCPDS Card No. 35-0270) [22] and orthorhombic structure WO_3, (JCPDS card 20-1324) [23].

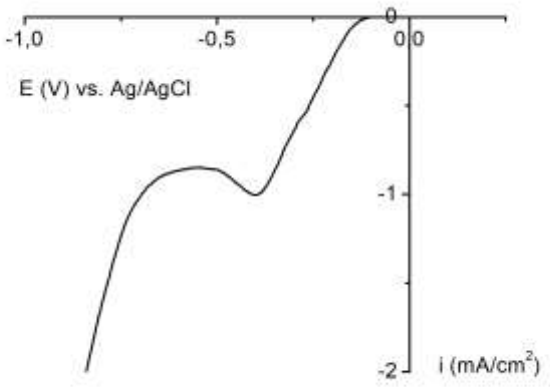

Fig. 2. Voltammetry of the process of obtaining Cu_2O from a solution ($CuSO_4$- 0.05 mol / l, citric acid 2 mol / l, KOH -to pH = 10). Scan rate 5 mV/s.

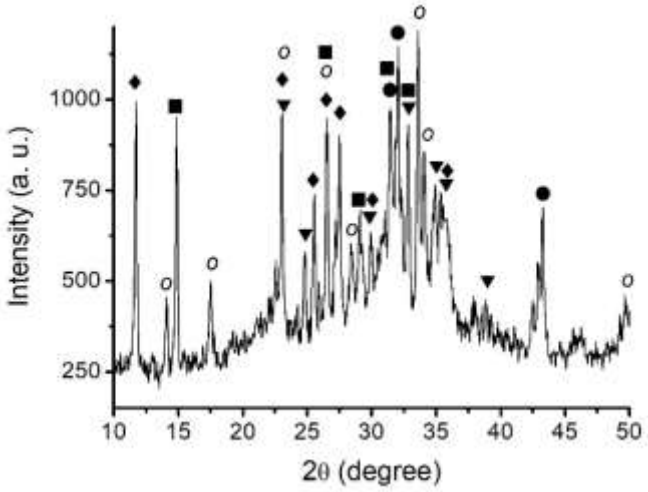

Fig. 3. XRD pattern of $CuWO_4$•WO_3 sample where ■- hydrated form of monoclinic $CuWO_4 \cdot 2H_2O$, ● – undeciphered tungstate structure [20], ▼- monoclinic WO_3•$2H_2O$, o- orthorhombic WO_3 •$0.33H_2O$, ■- orthorhombic structure tungsten trioxide

To assess the stability of the obtained bismuth and copper tungstate films as an electrochromic material, they were cycled in the galvanostatic mode with a current from +2.5 to -2.5 mA/cm^2 in 1 M $LiClO_4$ in propylene carbonate solutions while measuring light transmission (Fig. 4) . The comparison of the cycling rate of bismuth and copper tungstates with tungsten trioxide showed different rates of activity for the samples. Also, the comparison of the kinetics of color change processes of electrochromic films of copper and bismuth tungstates with tungsten trioxide showed that in the WO_3, Bi_2WO_6•WO_3, $CuWO_4$•WO_3 series, lithium intercalation in the films slows down. As can be seen from Fig. 4, the change in the light transmittance over the same period of time in three samples slows down in the series WO_3 (curve 1), Bi_2WO_6•WO_3 (curve 2) and $CuWO_4$•WO_3 (curve 3), which is due to the mobility of ions in these structures [24]. In the series WO_3, Bi_2WO_6•WO_3 and $CuWO_4$•WO_3, the highest mobility of charge carriers is observed in amorphous WO_3 films of 20 cm^2 /V.s [24], the lowest in $CuWO_4$ 0.006 cm^2 /V.s [25]. Since the effect of an electric field accelerates electrochromic processes only in those materials in which there are no significant obstacles to the intercalation of ions and the injection of electrons into the films, the materials whose composition includes oxides with the lowest mobility of charge carriers will

have the lowest lithium diffusion rate. At the same time, in the films of Bi_2WO_6•WO_3 and $CuWO_4$•WO_3 tungstates, a partial reverse reduction of oxide compounds of bismuth and copper to lower oxides is observed in comparison to tungsten trioxide. The results obtained show that differences in spectral characteristics are observed in composite films, which is expressed by the shift of the absorption band to the region of shorter wavelengths.

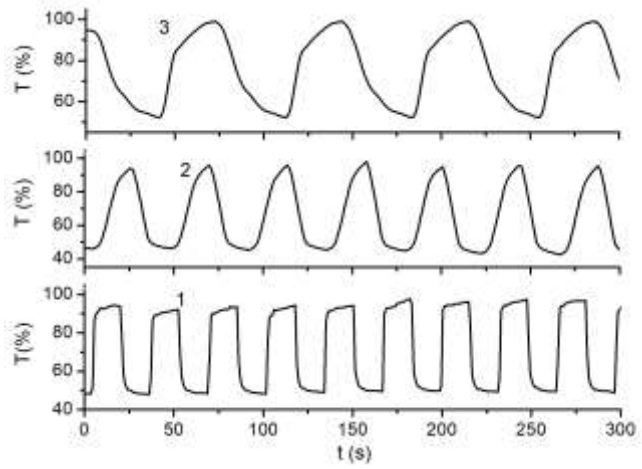

Fig. 4. Cyclic dependences of light transmittance for WO_3 films (1), Bi_2WO_6•WO_3 (2) $CuWO_4$•WO_3 (3) in the galvanostatic mode with a current of 2.5 and -2.5 (mA/cm2) (λ = 1000 nm)

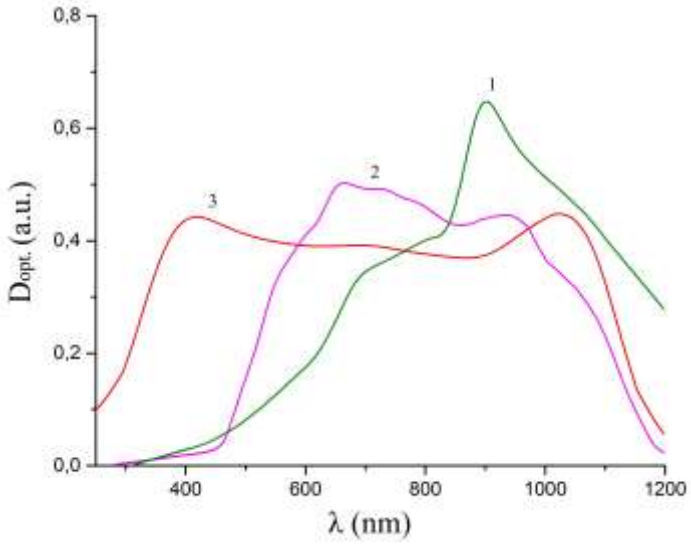

Fig. 5. Optical spectra of electrochromic coloration for WO_3 (1) Bi_2WO_6•WO_3 (2) $CuWO_4$•WO_3 (3) at j=-2.5 mA/cm^2 in 1 M $LiClO_4$ in propylene carbonate solution.

Fig. 5 shows the spectral characteristics of light transmittance of colored films of copper bismuth tungstates and tungsten trioxide. From Fig. 5 curve 1 it follows that for tungsten trioxide the absorption maximum is within λ=1000 nm. For bismuth tungstate obtained by electrodeposition, the absorption maximum occurs at 650 nm. And for $CuWO_4$ film with lithium intercalation, an even greater shift of the absorption band to λ=400 nm is observed. The comparison of the spectral characteristics of $CuWO_4$•WO_3, Bi_2WO_6•WO_3 and WO_3 showed that other oxide components besides WO_3 contribute to the color of the film. The analysis of literature data found that the transition from Cu^{2+} to Cu^{+} in copper oxide compounds is accompanied by the appearance of an absorption band at 400 nm [26] as in Fig. 4,

curve 3. And the partial reversible electrochemical reduction of Bi_2O_3 during Li^+ intercalation leads to the decrease in the transmission (increase in absorption) of light in the 550-650 nm range [27], which is also observed in our case in fig. 5, curve 2. Thus, in addition to the absorption band of tungsten trioxide, which falls mainly on the IR region (Fig. 5, curve 1), additional absorption bands appear in the visible part of the spectrum. This fact reveals that the use of metal tungstates is promising, provided that the intercalation of lithium into oxide components is sufficiently large.

Conclusions

By using of the combined chemical and electrochemical methods WO_3, Bi_2WO_6•WO_3 and $CuWO_4$•WO_3 films were synthesized. The study into the light transmission kinetics and spectral characteristics of electrochromic coloration revealed some differences in electrochromic processes in these films. It was found that in the series of WO_3, Bi_2WO_6•WO_3, $CuWO_4$•WO_3 there is a slowing down of lithium intercalation in films. This is due to diffusion limitations in the process of coloring complex oxides of Bi, Cu, and W. The spectral characteristics of electrochromic coloration Bi_2WO_6•WO_3 and $CuWO_4$•WO_3 also differ from WO_3, in that, in addition to tungsten trioxide, the contribution to light absorption is also made by oxides of Bi and Cu, which also partially are reduced by lithium in the process of their coloring. From this, it can be concluded that tungstates of metals can become effective electrochromic materials with an additional absorption band.

References

1. Li H., Firby C., Elezzabi A. Rechargeable aqueous hybrid Zn^{2+}/Al^{3+} electrochromic batteries. *Joule.* 2019, no. 3, pp. 2268-2278.
2. Li H., McRae L., Firby C., Elezzabi A. Recharge able aqueous electrochromic batteries utilizing Ti-substituted tungsten molybdenum oxide based Zn^{2+} ion intercalation cathodes *Adv Mater*. 2019, no. 31, pp. 1807065-1807210.
3. Zhang S., Cao S., Zhang T. Overcoming the technical challenges in Al anode-based electrochromic energy storage windows. *Small Methods.* 2020, no. 4, pp. 1900545-1900706.
4. Ma D., Shi G., Wang H., Zhang Q., Li Y. Controllable Growth of High-Quality Metal Oxide/Conducting Polymer Hierarchical Nanoarrays with Outstanding Electrochromic Properties and Solar-heat Shielding Ability. *J. Mater. Chem. A*, 2014, no. 2, pp. 13541-13549.
5. Lee S., Choi D., Kang S., Yang W., Nahm S., Han S., Kim T. VO_2/WO_3-Based Hybrid Smart Windows with Thermochromic and Electrochromic Properties. *ACS Sustainable Chem. Eng.*, 2019, no. 7, pp. 7111-7117.
6. Yuan C., Lin H., Lu H., Xing E., Zhang Y. Anodic deposition and capacitive property of nano-$WO_3 \cdot H_2O/MnO_2$ composite as supercapacitor electrode material. *Mater. Lett*. 2015, no. 148, pp. 167-170.
7. Nishiyamaa K., Matsuo R., Sasano J., Yokoyama S., Izaki M. Solid state tungsten oxide hydrate/tin oxide hydrate electrochromic device prepared by electrochemical reactions. *AIP Adv.* 2017, no. 7, pp. 035004-035005.
8. Santos L., Neto J., Crespo A., Baião P., Barquinha P., Pereira L., Martins R., Fortunato E. Electrodeposition of WO_3 Nanoparticles for Sensing Applications. In: Aliofkhazraei M. (ed) Electroplating of Nanostructures. *Intech Open*. 2015, no. 10, pp. 5772-61216.
9. Mineo G., Ruffino F., Mirabella S., Bruno E. Investigation of WO_3 Electrodeposition Leading to Nanostructured Thin Films. *Nanomaterials.* 2020, no. 10, pp. 1493-1505.
10. Esmail A., Hashem H., Soltan S., Hammam M., Ramadan A. Thickness dependence of electro-optical properties of WO_3 films as an electrochromic functional material for

energy-efficient applications. *Phys. Status Solid. A*, 2016, no. 214, pp. 1-9.
11. Khanapuram U., Bhat S., Aryasomayajula S. Electrochromic device with Magnetron sputtered Tungsten Oxide (WO_3) and nafion membrane: performance with varying Tungsten Oxide thickness - A report. *Mater. Res. Express*. 2019, no. 6, pp. 045513-045514.
12. Meulenkamp E. Mechanism of WO_3 electrodeposition from peroxy-tungstate solution. *Journal of the Electrochemical Society*. 2019, no. 144, pp. 1664-1672.
13. Krasnov Yu., Volkov S., Kolbasov G. Optical and kinetic properties of cathodically deposited amorphous tungsten oxide films. *J. NonCryst Solids*. 2006, no. 352, pp. 3995-4002.
14. Campos W., Nobre F. High Photocatalytic Activity under Visible Light for a New Morphology of Bi_2WO_6 Microcrystals. *Catalysts*. 2019, no. 9, pp. 667-668.
15. Mulik R. Hydrothermal synthesis of tungsten oxide (WO_3) for the detection of NO_2 gas. *17th International Meeting on Chemical Sensors*. 2018, pp. 531– 532.
16. Hssi A., Atourki L., Labchir N., Ouafi M., Abouabassi K., Elfanaoui A., Ihlal A., Bouabid K. Optical and dielectric properties of electrochemically deposited p-Cu_2O films. *Mater. Res. Express*. 2020, no. 7, pp. 16424-16425.
17. Yagi S. Potential-pH Diagrams for Oxidation-State Control of Nanoparticles Synthesized via Chemical Reduction. In: Moreno-Piraján JC (ed) Thermodynamics - Physical Chemistry of Aqueous Systems. *Intech Open*. 2011, no. 10, pp. 5772-21548.
18. Rezaie H., Hashempour M., Razavizadeh H., Mehrjoo H., Salehi M., Ardestani M. Investigation on Fabrication of W-Cu Nanocomposite via a Thermochemical Co-Precipitation Method and its Consolidation Behavior. *J. Nano Res*. 2010, no. 11, pp. 57-66.
19. Li Y., Wang N., Xu J., Liu Z., Yu H. Significant effect of advanced catalysts Co_3S_4 modified $CuWO_4{\cdot}2H_2O$ under visible light condition photocatalytic hydrogen production *J. Nanopart Res.* 2019, no. 21, pp. 80-81.
20. Kavitha B., Karthiga R. Synthesis and characterization of $CuWO_4$ as nano-adsorbent for removal of Nile blue and its antimicrobial studies. *J. Mater. Environ. Sci*. 2020, no. 11, 57-68.
21. Liang L., Zhang J., Zhou Y., Xie J., Zhang X., Guan M., Pan B., Xie Y. High-performance flexible electrochromic device based on facile semiconductor-to-metal transition realized by $WO_3{\cdot}2H_2O$ ultrathin nanosheets. *Sci. Rep*. 2013, no. 3, pp. 1936-1937.
22. Gao X., Yang C., Xiao F., Zhu Y., Wang J., Su X. $WO_3{\cdot}0.33H_2O$ nanoplates: Hydrothermal synthesis, photocatalytic and gas-sensing properties. *Mater. Lett.* 2012, no. 84, pp. 151-153.
23. Kadam A., Patil S. Polyaniline globules as a catalyst for WO_3 nanoparticles for supercapacitor application. *Mater. Res. Express*. 2018, no. 5, pp. 085036-085037.
24. Saenger M., Hoing T., Robertson B., Billa R., Hofmann T., Schubert E., Schubert M. Polaron and phonon properties in proton intercalated amorphous tungsten oxide thin films. *Physical Review B*. 2008, no. 78, pp. 245205-245211.
25. Songcan W., Lianzhou W. Recent progress of tungsten-and molybdenum-based semiconductor materials for solar-hydrogen production. *Tungsten*. 2019, no. 1, pp. 19-45.
26. Yang Y., Xu D., Wu Q. Cu_2O/CuO Bilayered Composite as a High-Efficiency Photocathode for Photoelectrochemical Hydrogen Evolution Reaction. *Sci. Rep*. 2016, no. 6, pp. 35158-35159.
27. Fan H., Yan W., Ding Y., Bao Z. Using Flame-Assisted Printing to Fabricate Large Nanostructured Oxide Thin Film for Electrochromic Applications. *Nanoscale Res. Lett.* 2020, no. 15, pp. 218-219.

СРАВНИТЕЛЬНЫЙ АНАЛИЗ ЭЛЕКТРОХРОМНЫХ СВОЙСТВ ТОНКИХ ПЛЕНОК $CuWO_4 \bullet WO_3$, $Bi_2WO_6 \bullet WO_3$ И WO_3

В.О. Смилык, С.С. Фоманюк*, И.А. Русетский, М.О. Данилов , Г.Я. Колбасов

Институт Общей и Неорганической Химии им. В.И. Вернадского НАН Украины
Пр.Палладина, 32-34, Киев 03142, Украина
** e–mail: fomanyuk@gmail.com*

Аннотация: Пленки $Bi_2WO_6 \bullet WO_3$, $CuWO_4 \bullet WO_3$ and WO_3 были синтезированы комбинированным химическим и электрохимическим методами. Изучение кинетики светопропускания и спектральных характеристик электрохромного эффекта позволило установить некоторые различия электрохромных процессов в этих пленках. Показано, что в ряду WO_3, $Bi_2WO_6 \bullet WO_3$, $CuWO_4 \bullet WO_3$ происходит замедление интеркаляции лития в пленки, что связано с диффузионными ограничениями в процессе окрашивания сложных оксидов Bi, Cu и W. Характеристики электрохромного окрашивания $Bi_2WO_6 \bullet WO_3$ и $CuWO_4 \bullet WO_3$ также отличаются от WO_3 тем, что, помимо триоксида вольфрама, вклад в поглощение света вносят также оксиды Bi и Cu, которые также частично восстанавливаются литием в процессе их окраски. Сделан вывод о том, что вольфраматы металлов могут стать эффективными электрохромными материалами, имеющими дополнительную полосу поглощения в видимой области спектра.
Ключевые слова: электрохромизм, вольфраматы металлов, электрохромные композиты

$CuWO_4 \bullet WO_3$, $Bi_2WO_6 \bullet WO_3$ VƏ WO_3 NAZİK TƏBƏQƏLƏRİN ELEKTROXROM XÜSUSİYYƏTLƏRİNİN MÜQAYİSƏLİ TƏHLİLİ

V.O. Smilık, S.S. Fomanyuk*, I.A. Rusetskiy, M.O. Danilov, Q.Ya. Kolbasov

Ukrayna Milli Elmlər Akademiyası,
V.İ. Vernadsky ad. Ümumi və Qeyri-üzvi Kimya İnstitutu
** e–mail: fomanyuk@gmail.com*

Xülasə: $Bi_2WO_6 \bullet WO_3$, $CuWO_4 \bullet WO_3$ və WO_3 nazik təbəqələr kombinə edilmiş kimyəvi və elektrokimyəvi üsullarla sintez edilmişdir. İşığın ötürülməsinin kinetikasının və elektroxrom effektinin spektral xüsusiyyətlərinin öyrənilməsi bu plyonkalarda elektroxrom proseslərdə bəzi fərqlər müəyyən etməyə imkan vermişdir. Göstərilmişdir ki, WO_3, $Bi_2WO_6 \bullet WO_3$, $CuWO_4 \bullet WO_3$ sırasında litiumun təbəqələrə interkalyasiyası ləngiyir, bu da Bi, Cu və W mürəkkəb oksidlərinin rənglənməsi prosesində diffuziya məhdudiyyətləri ilə əlaqələndirilir. Belə nəticəyə gəlinib ki, işıq spektrinın görünən hissəsində əlavə udma zolağın olması səbəbindən metal volframatlar effektiv elektroxrom materiallar ola bilərlər.
Açar sözlər: elektroxromizm, metal volframatlar, elektroxrom kompozitlər